CFD Letters

Journal homepage:
https://semarakilmu.com.my/journals/index.php/CFD_Letters/index
ISSN: 2180-1363

Three-dimensional MHD Mixed Convention Upper Convective Flow of Maxwell Fluid Throughout the Past in Thermophoresis and Brownian Motion with the Effects of Diffusion Thermo and Thermal Diffusion Utilizing Nonlinear Radiative Heat Flux

Rameswara Reddy Yeddula[1,*], Srinivasan Donti Ratnam[2]

[1] Department of Mechanical engineering, JNTUA College of Engineering Pulivendula-516390, Constitute College of Jawaharlal Nehru Technological University Anantapur , Ananthapuramu, A.P, India
[2] Department of Mechanical Engineering, JNTUA College of Engineering Kalikiri-517234, Constitute college of Jawaharlal Nehru Technological University Anantapur, Ananthapuramu, A.P, India

ARTICLE INFO

Article history:
Received 31 July 2023
Received in revised form 25 August 2023
Accepted 20 September 2023
Available online 10 January 2024

Keywords:
Thermal Radiation; MHD; Maxwell fluid; Brownian motion; thermophoresis

ABSTRACT

This article aims to investigate the impact of nanoparticles and magnetohydrodynamics (MHD) on the transfer of heat and mass using a three-dimensional upper-convected Maxwell (UCM) nanofluid flow across a stretched surface. A nonlinear radiative heat flow was included in formulating the equation that describes energy. The nonlinear partial differential equations of the issue are transformed into ordinary differential equations utilizing the similarity transformation. These equations are then solved using the well-known shooting approach in conjunction with the Runge-Kutta integration process of order four. To increase the dependability of our findings make use of the MATLAB. On the velocities, temperatures, and concentrations of the particles, the graphical and numerical representations of the effects of the main parameters, such as the Dufour parameter, the Brownian motion parameter, the Prandtl number, the thermophoresis parameter, and the magnetic parameter, are presented. It has been shown that the flow velocity decreases as a function of both the linear and nonlinear thermal radiation parameters. In addition, increasing values of the Brownian motion parameter have the effect of reducing the nanoparticle concentration profile, the same behavior has observed in the case of thermal diffusion and Diffusion thermo parameters.

1. Introduction

In resent few years, study of the non-Newtonian fluids is curiously expanded because of their extensive dimension, useful technological and industrial applications. Shampoos, blood at low shear rate, soaps, apple sauce, mud, chyme, sugar solution, emulsion, etc are some real life examples of non-Newtonian fluids. In polymer, chemical and biomedical industries, the importance of non-Newtonian fluids cannot be denied. In almost all the industrial and biological fluids, the relationship

* *Corresponding author.*
*E-mail address: yrameswarareddy.mech@jntua.ac.in (*Rameswara Reddy Yeddula*)*

https://doi.org/10.37934/cfdl.16.5.135153

between the rate of deformation and the stress is not linear. The sole properties of all non-Newtonian fluids cannot be completely described by any concrete single equation/relation. Due to this, researchers have suggested various mathematical models of non-Newtonian fluids. Amongst these models, Maxwell fluids and viscoelastic fluids have ample range of industrial applications such as glass blowing, extrusion of polymer sheets, manufacturing of plastic films, hot rolling, crystal growing etc. The viscoelastic fluid models such as second order and/or Walter-B fluid models are recommended for fluids having small level of elasticity [1]. These fluid models violate some established rules of thermodynamics [2]. For highly viscoelastic polymers, second grade fluid models with high Deborah number do not give the meaningful results [3, 4], which reduces their significance in the polymer industry. Consequently, some more realistic fluid models, such as Oldroyd-B or upper-convected Maxwell fluid models have been considered for the application purpose [5]. Indeed these two models for viscoelastic fluid flow have been studied on stretching and non-stretching sheets. Ali and Ashrafi [6] have investigated the upper convected Maxwell fluid with high Weissenberg number over a linearly stretching sheet. Velocity and heat transfer analysis of the fluid flow is carried out by using the shooting technique. Mushtaq *et al.,* [7] analyzed the Sakiadis flow of upper-convected Maxwell fluid through a stretching sheet using Cattaneo-Christov model. Omowaye and Animasaum [8] studied the MHD UCM (upper convected Maxwell) fluid over a melting surface subject to thermal stratification with variable thermo-physical properties. They concluded that velocity profile is enhanced for the higher values of Deborah number. Krupalakshmi *et al.,* [9] found the numerical solution of UCM fluid in the existence of dust particles over convectively heated stretching sheet. They incorporated the magnetic field and discussed the effects of viscous dissipation, non-linear thermal radiation, and heat source/sink. Waini *et al.,* [10] considered the inclined magnetic field through a continuously stretched sheet for the study of heat and fluid flow of UCM fluid. They concluded that the magnetic field's strength is enhanced when the inclination of the aligned magnetic field is high, and resultantly it increases the temperature and reduces the velocity of the fluid. Bilal *et al.,* [11] Have Studied on MHD 3d Upper Convected Maxwell Fluid Flow With thermophoretic effect Using Nonlinear Radiative Heat Flux.

The research on stagnation point flow of nanofluid over stretching surface has different applications in industries and technology. Raghunath *et al.,* [12] have studied processing to pass unsteady MHD flow of a second-grade fluid through a porous medium in the presence of radiation absorption exhibits Diffusion thermo, hall and ion slip effects. Raghunath *et al.,* [13] have studied Influence of MHD mixed convection flow for maxwell nanofluid through a vertical cone with porous material in the existence of variable heat conductivity and diffusion. Raghunath *et al.,* [14] Radiation absorption on MHD Free Conduction flow through porous medium over an unbounded vertical plate with heat source. Li *et al.,* [15] have studied Effects of activation energy and chemical reaction on unsteady MHD dissipative Darcy–Forchheimer squeezed flow of Casson fluid over horizontal channel**.** Suresh Kumar [16] have expressed Numerical analysis of magneto hydrodynamics Casson nanofluid flow with activation energy, Hall current and thermal radiation. Aruna *et al.,* [17] have possessed an unsteady MHD flow of a second-grade fluid passing through a porous medium in the presence of radiation absorption exhibits Hall and ion slip effects.

Thermal radiation is the phenomenon of energy or heat transmission in the form of electromagnetic waves. The thermal radiation is significant in the high-temperature variance case among the ambient fluid and boundary surface. In engineering and physics, radiative impacts play an essential role. The effects of radiation heat transfer on various flows are essential in high-temperature and space technology processes. The effects of radiation are important in monitoring heat transmission in the polymer industries, where the final product quality is influenced by heat controlling variables to some extent. Also, the radiative impacts are significant in missiles, aircraft,

gas turbines, solar radiations, space vehicles, liquid metal fluids, MHD accelerators, and nuclear power plants. The impact of nonlinear thermal radiation on the Sakiadis flow was analysed by Pantokratoras and Fang [18]. Raghunath *et al.,* [19] have studied Hall current and thermal radiation effects of 3D rotating hybrid nanofluid reactive flow via stretched plate with internal heat absorption.

The Soret effect is associated with mass flux phenomena induced by heat diffusion, while the Dufour effect is related to the energy flux generated by the solute difference. The Soret impact is used to cope with concentrations of gases having lighter and medium molecular mass. Heat and mass transfer via the Soret and Dufour phenomena are significant in a wide range of industrial and engineering applications, like geosciences multi component melts, groundwater pollutant migration, solidification of binary alloys, chemical reactors, space cooling, isotope separation, oil reservoirs, and mixtures of gases. Raghunath *et al.,* [20] have analysed unsteady magneto-hydro-dynamics flow of Jeffrey fluid through porous media with thermal radiation, Hall current and Soret effects. Raghunath [21] has studied Study of Heat and Mass Transfer of an Unsteady Magnetohydrodynamic Nanofluid Flow Past a Vertical Porous Plate in the Presence of Chemical Reaction, Radiation and soret Effects. Raghunath *et al.,* [22] has analyzed Diffusion Thermo and Chemical Reaction Effects on Magnetohydrodynamic Jeffrey Nanofluid over an Inclined Vertical Plate in the Presence of Radiation Absorption and Constant Heat Source. Maatoug *et al.,* [23] have expressed Variable chemical species and thermo-diffusion Darcy–Forchheimer squeezed flow of Jeffrey nanofluid in horizontal channel with viscous dissipation effects. Omar *et al.,* [24] have possessed Hall Current and Soret Effects on Unsteady MHD Rotating Flow of Second-Grade Fluid through Porous Media under the Influences of Thermal Radiation and Chemical Reactions. Deepthi *et al.,* [25] have discussed Recent Development of Heat and Mass Transport in the Presence of Hall, Ion Slip and Thermo Diffusion in Radiative Second Grade Material: Application of Micromachines.

All the above investigators disregard three-dimensional upper-convected Maxwell (UCM) nanofluid flow over a stretching surface, which has been considered to examine the effects of nanoparticles and magnetohydrodynamics (MHD) on the heat and mass transfer in the presence of soret and Dufour effects. Non-linear radiative heat flux is incorporated in the formulation of the energy equation. Similarity transformation reduces the non-linear partial differential equations of the problem to the ordinary differential equations, which are then solved by the well-known shooting technique through the Runge-Kutta integration procedure of order four. The built-in MATLAB function bvp4c is also used to improve the reliability of our results.

2. Formulation of the Problem

A steady incompressible upper convected Maxwell nanofluid over a bilinear stretching surface in the positive xy-plane is considered to investigate the behavior of temperature and concentration. A uniform magnetic field of strength B_0 is applied normal to the flow i.e. in the z−direction. The induced magnetic field is ignored because of the assumption of the small Reynolds number. Applied magnetic field drags the magnetic field lines in the direction of the flow which interact with the induced current density to give rise a force known as the Lorentz force. Further, a non-linear thermal radiation is taken into account during the formulation of the energy equation. The stretching surface velocities in the x and y plane are considered as $U_w(x)$. = ax and $V_w(y)$. = by respectively as shown in Figure 1. Under these assumptions, the governing equations of time-independent and incompressible boundary layer flow nanofluid over stretching sheet are given by:

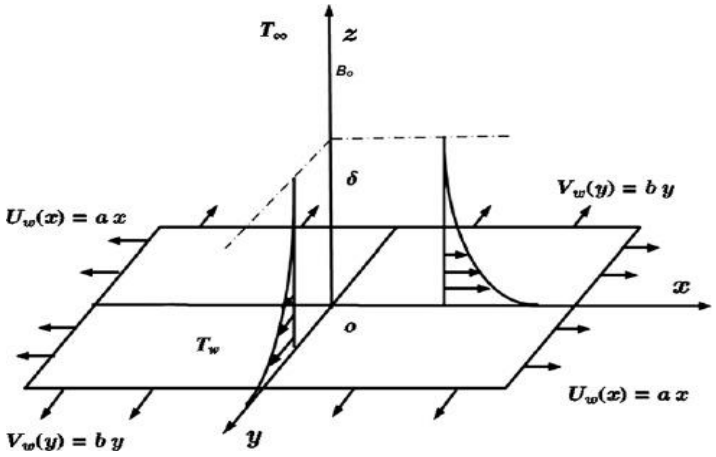

Fig. 1. Physical configuration of the problem

$$\frac{\partial u}{\partial x}+\frac{\partial v}{\partial y}+\frac{\partial w}{\partial z}=0 \tag{1}$$

$$u\frac{\partial u}{\partial x}+v\frac{\partial u}{\partial y}+w\frac{\partial u}{\partial z}=\nu\frac{\partial^2 u}{\partial x^2}-\lambda\left(\begin{array}{l}u^2\dfrac{\partial^2 u}{\partial x^2}+v^2\dfrac{\partial^2 u}{\partial y^2}+w^2\dfrac{\partial^2 u}{\partial z^2}+\\ 2uv\dfrac{\partial^2 u}{\partial x\,\partial y}+2uw\dfrac{\partial^2 u}{\partial x\,\partial z}+2vw\dfrac{\partial^2 u}{\partial y\,\partial z}\end{array}\right)- \left(\frac{\sigma B_0^2}{\rho}\right)\left(u+\lambda w\frac{\partial u}{\partial z}\right)+g_C\beta_T(T-T_\infty)+g_C\beta_C(C-C_\infty) \tag{2}$$

$$u\frac{\partial v}{\partial x}+v\frac{\partial v}{\partial y}+w\frac{\partial v}{\partial z}=\nu\frac{\partial^2 v}{\partial z^2}-\lambda\left(\begin{array}{l}u^2\dfrac{\partial^2 v}{\partial x^2}+v^2\dfrac{\partial^2 v}{\partial y^2}+w^2\dfrac{\partial^2 v}{\partial z^2}+\\ 2uv\dfrac{\partial^2 v}{\partial x\,\partial y}+2uw\dfrac{\partial^2 v}{\partial x\,\partial z}+2vw\dfrac{\partial^2 v}{\partial y\,\partial z}\end{array}\right)-\left(\frac{\sigma B_0^2}{\rho}\right)\left(v+\lambda w\frac{\partial v}{\partial z}\right) \tag{3}$$

$$u\frac{\partial T}{\partial x}+v\frac{\partial T}{\partial y}+w\frac{\partial T}{\partial z}=\alpha\left(\frac{\partial^2 T}{\partial z^2}\right)+\tau\left(D_B\frac{\partial C}{\partial z}\frac{\partial T}{\partial z}+\frac{D_T}{T_\infty}\left(\frac{\partial T}{\partial z}\right)^2\right)-\frac{1}{\rho C_p}\frac{\partial q_r}{\partial z}+\frac{D_m k_T}{c_s c_p}\frac{\partial^2 C}{\partial z^2} \tag{4}$$

$$u\frac{\partial C}{\partial x}+v\frac{\partial C}{\partial y}+w\frac{\partial C}{\partial z}=\frac{D_m k_T}{T_m}\frac{\partial T^2}{\partial y^2}+D_B\left(\frac{\partial^2 C}{\partial z^2}\right)+\frac{D_T}{T_\infty}\frac{\partial^2 T}{\partial z^2} \tag{5}$$

For this flow, corresponding boundary conditions are the corresponding boundary conditions for the governing PDEs are

$$\begin{aligned} &u = u_w = ax, \quad v = v_w = b_y, \quad w = 0, \quad T = T_w, \quad C = C_w \quad \text{at } z = 0 \\ &u \to 0, \quad v \to 0, \quad w \to 0, \quad T \to T_\infty \quad C \to C_\infty \quad \text{as} \quad z \to \infty \end{aligned} \tag{6}$$

Dimensionless quantities are introduced to simplify the mathematical analysis of the problem by introducing the following similarity transformation used to transform the PDEs to dimensionless ODEs

$$u = ax\, f'(\eta),\ v = ay\, g'(\eta),\ w = -\sqrt{a\nu}\,(f(\eta) + g(\eta)),\ \eta = \sqrt{\frac{a}{\nu}}z,\ \theta(\eta) = \frac{T - T_\infty}{T_w - T_\infty},\ \phi(\eta) = \frac{C - C_\infty}{C_w - C_\infty} \tag{7}$$

The Rosseland approximation can be used for the radiative heat flux vector qr because there is also self-absorption in addition to emission for an optically thick fluid. Since the absorption coefficient is typically wavelength dependent and significant, we can use the Rosseland approximation. Therefore, the definition of qr is [26, 27].

$$q_r = -\frac{4\sigma^*}{3\mathrm{N}}\frac{\partial T^4}{\partial z} \tag{8}$$

T in Eq. (8) can be expressed as [27] since non-linear thermal radiation is being taken into consideration.

$$T = T_\infty\left((\theta_w - 1)\theta + 1\right). \tag{9}$$

Using Eq. (8) and Eq. (9)

$$q_r = -\frac{16\sigma^*}{3\mathrm{N}}T_\infty^3\left((\theta_w - 1)\theta + 1\right)^3\frac{\partial T}{\partial z} \tag{10}$$

Upon converting Eq. (2) through Eq. (5) to ordinary differential equations, Eq. (1) is identically satisfied:

$$\begin{aligned} f''' - f'^2 + \left(M^2\Lambda + 1\right)(f + g)f'' + Gr_x\theta + Gr_c\phi + 2\Lambda f'(f + g)f'' - \\ \Lambda f'(f + g)^2 f''' - M^2 f'' = 0 \end{aligned} \tag{11}$$

$$\begin{aligned} g''' - g'^2 + \left(M^2\Lambda + 1\right)(f + g)g'' + 2\Lambda g'(f + g)g'' - \\ \Lambda f'(f + g)^2 g''' - M^2 g'' = 0 \end{aligned} \tag{12}$$

$$\begin{aligned} \theta'' + \frac{4}{3}R_d\left[(1 + (\theta_w - 1)\theta)^3\theta'' + 3(\theta_w - 1)(1 + (\theta_w - 1)\theta)^2\theta'^2\right] + \\ \Pr(f + g)\theta' + \Pr N_b\left(\theta'\phi' + \frac{N_t}{N_b}\theta'^2\right) + \Pr D_u\phi' = 0 \end{aligned} \tag{13}$$

$$\phi'' + \Pr\ L_e\left(f+g\right)\phi' + L_e Sr\phi' + \frac{N_t}{N_b}\theta'' = 0 \tag{14}$$

The correlated Dimensionless boundary conditions (BCs) are

$$\begin{aligned} &f(0)=0,\quad f'(0)=1,\quad g(0)=0,\quad g'(0)=c,\quad \theta(0)=0,\quad \phi(0)=1 \qquad at \quad \eta=0 \\ &f'(\eta)\to 0,\quad g'(\eta)\to 0,\quad \theta(\eta)\to 0,\quad \phi(\eta)\to 0 \qquad as \quad \eta\to\infty \end{aligned} \tag{15}$$

In the equations that do not include dimensions, the important parameters are defined as

$$\begin{aligned} &M=\frac{\sigma B_0^2}{\rho a},\ \Pr=\frac{\nu}{\alpha}=\frac{\nu\rho C_p}{k},\ L_e=\frac{\alpha}{D_B}, N_b=\frac{\tau D_B\left(C_w-C_\infty\right)}{\nu},\quad N_t=\frac{\tau D_T\left(T_w-T_\infty\right)}{\nu T_\infty}, \\ &Du=\frac{D_M k_T\left(C_w-C_\infty\right)}{C_S C_p \nu a^2\left(T_w-T_\infty\right)}, R_d=\frac{4\sigma^* T_\infty^3}{kN}, c=\frac{b}{a}, \theta_w=\frac{T_w}{T_\infty}, Gr_x=\frac{g_c\beta_T\left(T_w-T_\infty\right)}{a^2 x}, \\ &Gr_c=\frac{g_c\beta_C\left(C_w-C_\infty\right)}{a^2 x}, S_r=\frac{D_m k_T\left(T_w-T_\infty\right)}{T_m\alpha_m\left(C_w-C_\infty\right)}. \end{aligned} \tag{16}$$

The local Nusselt number Nu_x, and the local Sherwood number Sh_x are the physical quantities of relevance that influence the flow. These numbers have the following definitions:

$$Nu_x=\frac{xq_w}{k\left(T_w-T_\infty\right)},\ Sh_x=\frac{x\,j_w}{D_B\left(C_w-C_\infty\right)} \tag{17}$$

Where wall heat flux and wall mass flux respectively given by

$$q_w=-k\left[\frac{\partial T}{\partial y}\right]_{z=0},\qquad j_w=-D_B\left[\frac{\partial C}{\partial y}\right]_{z=0} \tag{18}$$

The coefficient of Nusselt number, and the Sherwood number are all expressed in their non-dimensional versions in terms of the similarity variable as follows:

$$\mathrm{Re}_z^{1/2}\ Nu_z=-\left(1+\frac{4}{3}R_d\theta_w^3\right)\theta'(0),\ \ \mathrm{Re}_z^{1/2}\ Sh_z=-\phi'(0) \tag{19}$$

3. Solution Methodology

The system of non-linear ODEs Eq. (11)-(14) subject to the boundary conditions Eq. (15) has been solved by the shooting method for various values of the involved parameters. We observed through graphs that for η > 7, there is no significant variation in the behavior of solutions. Therefore, on the basis of such computational experiments, we are pondering [0, 7] as the domain of the problem instead of [0, ∞). We denote f by y_1, g by y_4, θ by y_7 and ϕ by y_9 for converting the boundary value

problem Eq. (11)-(14) to the following initial value problem consisting of 10 first order differential equations.

$$y_1' = y_2,$$

$$y_2' = y_3,$$

$$y_3' = \frac{1}{1-\Lambda(y_1+y_4)^2}\left(y_2^2 - (M^2\Lambda+1)(y_1+y_4)y_3 + 2\Lambda y_2 y_3(y_1+y_4) - Gr_x y_7 - Gr_c y_9 + M^2 y_2\right),$$

$$y_4' = y_5,$$

$$y_5' = y_6,$$

$$y_6' = \frac{1}{1-\Lambda(y_1+y_4)^2}\left(y_5^2 - (M^2\Lambda+1)(y_1+y_4)y_6 - 2\Lambda y_5 y_6(y_1+y_4) + M^2 y_5\right),$$

$$y_7' = y_8,$$

$$y_7' = \frac{-3}{3+4R_d(1+(\theta_w-1)y_7)^3}\left(\begin{array}{l}\left(4Rd(\theta_w-1)(1+(\theta_w-1)y_7)^2\right)y^2{}_8 + \\ \Pr\left((y_1+y_4)y_8 + \Pr\left(y_8 y_{10} + \frac{N_t}{N_b}y_8^2\right) + \Pr Du y_{10}\right)\end{array}\right)$$

$$y_9' = y_{10},$$

$$\phi'' + \Pr\ L_e\,(f+g)\phi' + L_e\,Sr\phi' + \frac{N_t}{N_b}\theta'' = 0$$

$$y_{10}' = -\Pr\ L_e\,(y_1+y_4)y_{10} - L_e Sr y_{10} - \frac{N_t}{N_b}y_8'$$

To solve the above initial value problem arising in the shooting method, Runge Kutta method of order four is used with $\varepsilon = 10^{-7}$.

4. Results and Discussion

We have obtained the solution of Eq. (11) - (14) Subject to the Eq. (15) with the help of MATLAB software by its bvp4c methodology. We have sketched graphs to examine the influence of numerous parameters appearing in equations for dimensionless velocity, temperature, and concentration. The parameter's ranges are taken as Sr=0.5, Grx=0.5, Grc=0.3, Le=1.0, Pr=0.2, M=2.0, c=0.5, Rd=1.0, Nb=0.8, Nt=1.2, Λ=0.3, Du=0.5.

Figures 2 and 3 depict the typical profiles of velocity and temperature for the magnetic parameter M. By increasing the magnetic parameter M, a drag force known as the Lorentz force also increases which resultantly reduces the velocity of the fluid and hence the rate of heat transfer is reduced and this leads to an increment in the temperature.

In Figures 4-7 the effects of the thermal Grashof Gxr and mass Grashof rc numbers on the tangential velocity $f''(\eta)$, the transverse velocity $g(\eta)$, are displayed respectively. As the Grashof number is a ratio of the buoyancy force to the viscous force and it appears due to the natural convection flow, so an increase in the tangential velocity as well as the transverse velocity of the fluid. It happens because of the fact that higher the Grashof number implies higher the buoyancy force which means higher the movement of the flow.

Figure 8 and Figure 9 reflect the impact of the Deborah number Λ, which is a ratio of the fluid relaxation time to its characteristic time scale on the velocity profiles. When the shear stress is applied on the fluid, the time in which it gains its equilibrium position is called relaxation time. This time is higher for the fluids having high viscosity. So an increase in the Deborah number may increase the viscosity of the fluid and hence the velocity decreases as shown in Figure 4 and Figure 5. The fluid becomes Newtonian if we consider $\Lambda = 0$ and its viscosity gradually increases with an increase in the Deborah number Λ. From Figure 9, it is also concluded that boundary layer thickness reduces for the upper convected Maxwell fluid. When Λ is increased, the hydrodynamic boundary layer thickness decreases. In Figure 10 and Figure 11, the effect of the variation in the Deborah number on the temperature $\theta(\eta)$ and the nanoparticle concentration $\phi(\eta)$ is displayed respectively. It is observed that the temperature and the concentration increase with an increase in the relaxation time. From this observation, we can conclude that the elastic force promotes the heat and the mass transfer in the upper-convected Maxwell nanofluid.

To see the variation in the temperature profile against the increasing values of the Prandtl number Pr, Figure 12 is plotted in which the increasing values of Prandtl number result in a thinner temperature boundary layer thickness. Fluids having larger Prandtl number have lower thermal diffusivity, and hence the temperature decreases. The same decreasing trend of Pr number on the mass concentration profile is observed in Figure 13. The influence of Brownian motion parameter on concentration and temperature profiles is depicted through Figure 14 and Figure 15. From the figures, it can be seen that as the values of Brownian motion parameter rises, the thermal boundary layer thickness increases and at the surface, the temperature gradient demises. But we witnessed an opposite result on the concentration profiles and concentration boundary layer thickness as Brownian motion parameter upsurges. Figures 16 and Figure 17 are devoted to demonstrate the impact of thermophoresis parameter on temperature and concentration profiles. From the figures, it is perceived that when thermophoresis parameter rises, there is an improvement of the thermal and concentration boundary layer thickness.

The temperature and nanoparticle concentration curves for different values of thermal radiation parameter are depicted in Figure 18 and Figure 19. From the graph, it is possible to observe that as the values of thermal radiation parameter upsurge, the temperature graph and the temperature boundary layer thickness are snowballing. In Figure 20 and Figure 21, the effect of the diffusion thermo parameter Rd on the temperature and nanoparticle concentration profiles. It is observed that the nanoparticle concentration decreases with an increment in Du, the reversal behavior has observed in the case of temperature.

Figure 22 and Figure 23 illustrate that the Soret number Sr decreases temperature profile while there is an increase in concentration profile and boundary layer thickness. Higher temperature difference and a lower concentration difference are observed because of increasing values of the Soret number. This variation in the temperature and concentration differences is liable for the

decrease in the temperature and an increase in the concentration. It is also noticed that the Dufour and Soret numbers have fairly contrary effects for temperature and nanoparticle concentration fields.

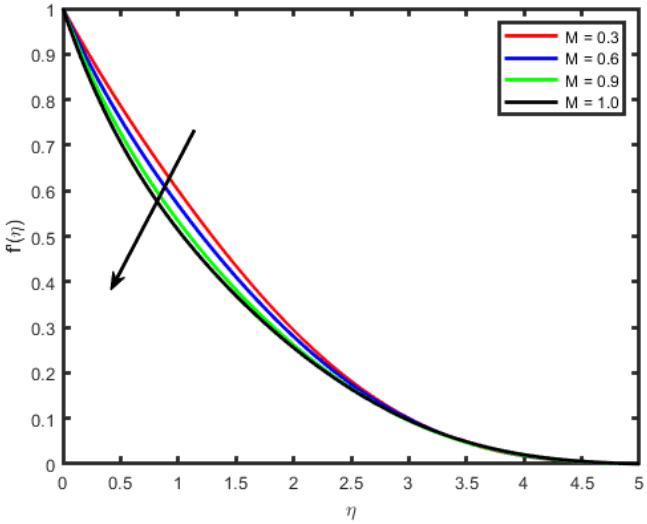

Fig. 2. Influence of M on f'(η)

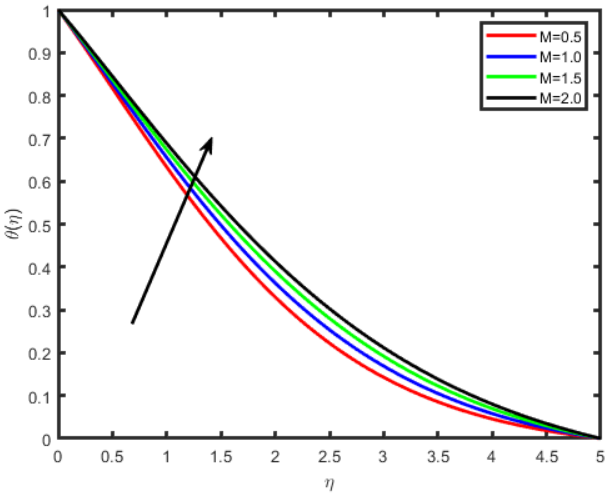

Fig. 3. Influence of M on θ(η)

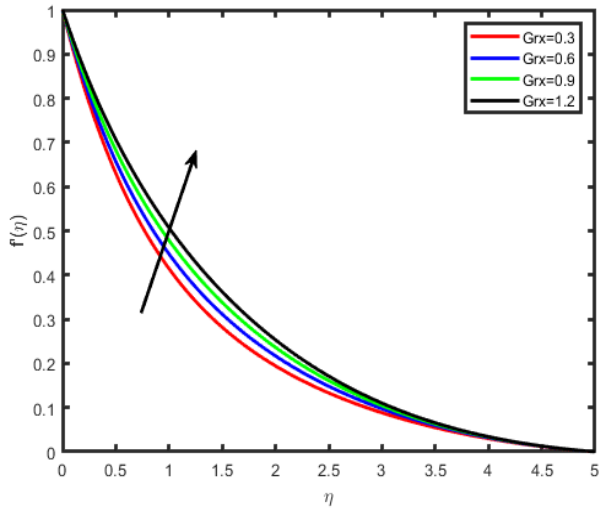

Fig. 4. Effect of Gr on f'(n)

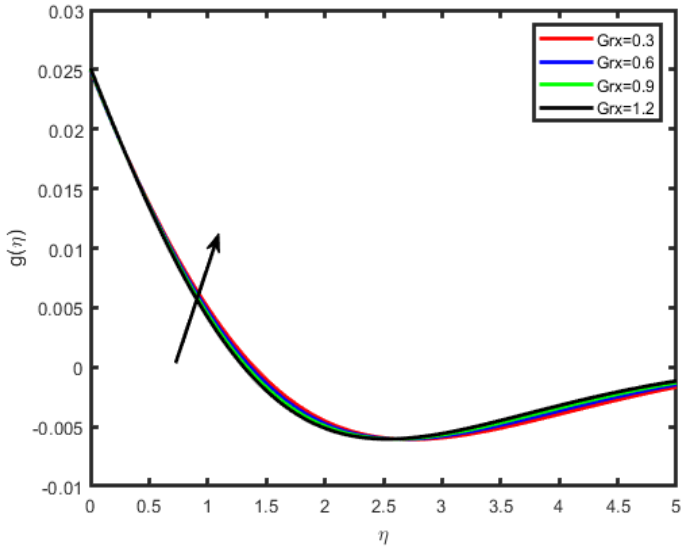

Fig. 5. Effect of Gr on g(n)

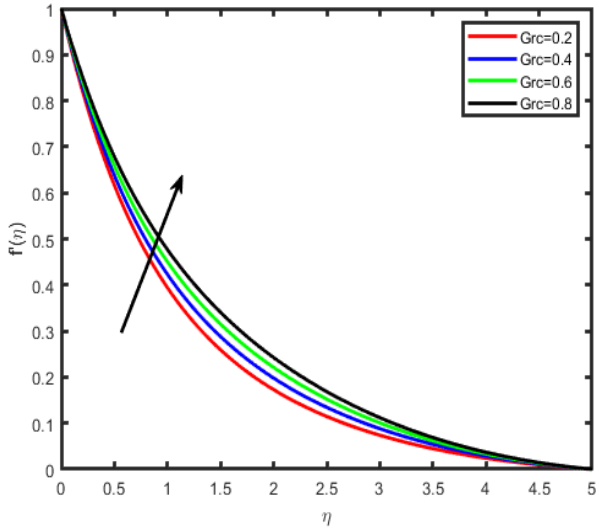

Fig. 6. Effect of Gm on f′(n)

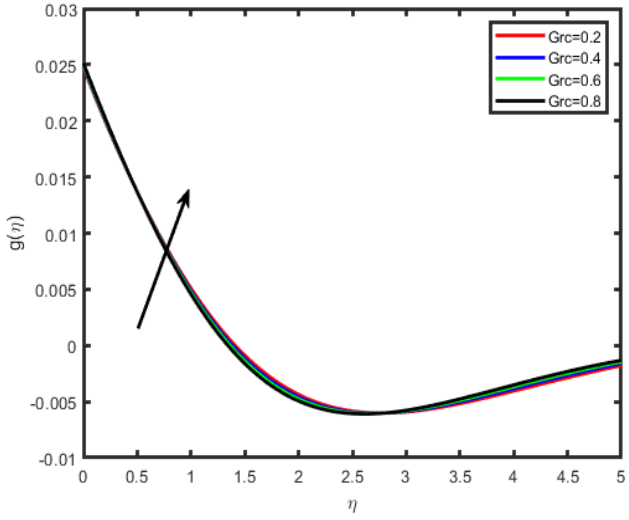

Fig. 7. Effect of Gm on g(n)

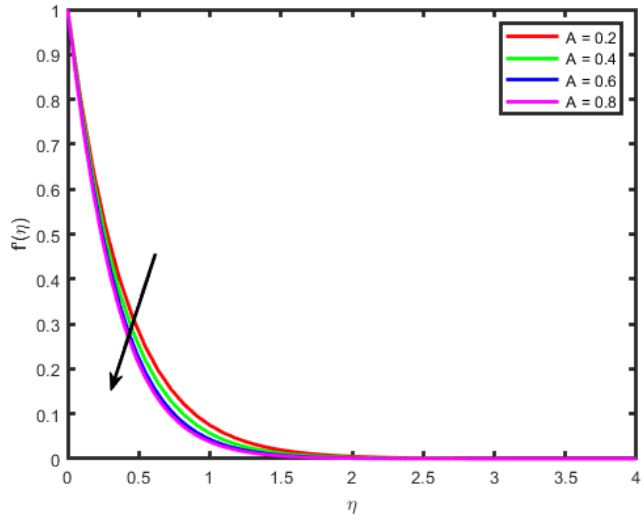

Fig. 8. Influence of Λ on f^{l}(η)

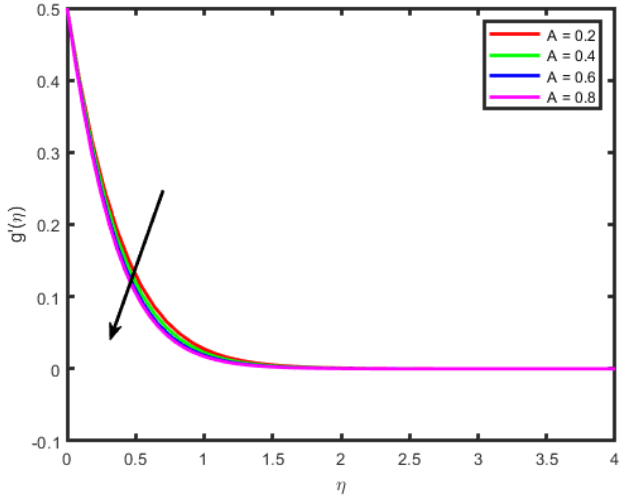

Fig. 9. Influence of Λ on g^{l}(η)

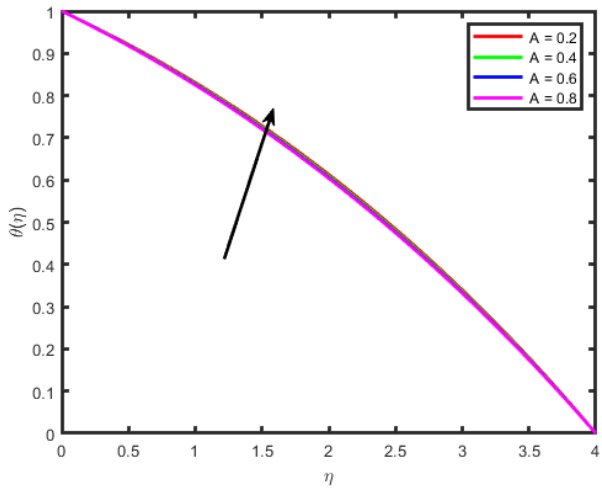

Fig. 10. Influence of Λ on θ(η)

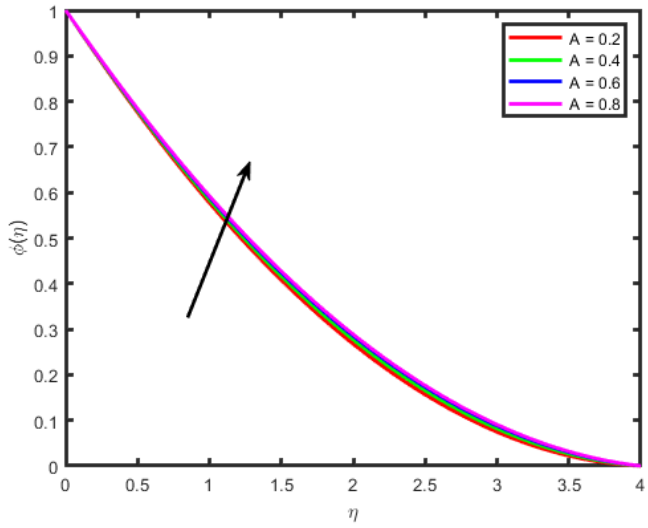

Fig. 11. Influence of Λ on ϕ(η)

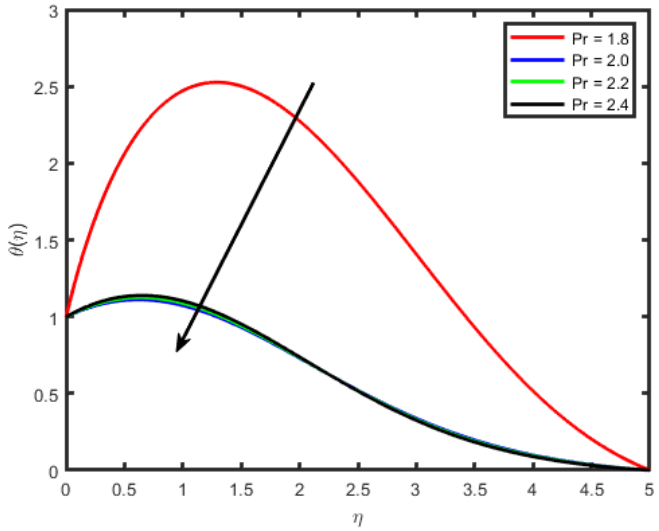

Fig. 12. Influence of Pr on θ(η)

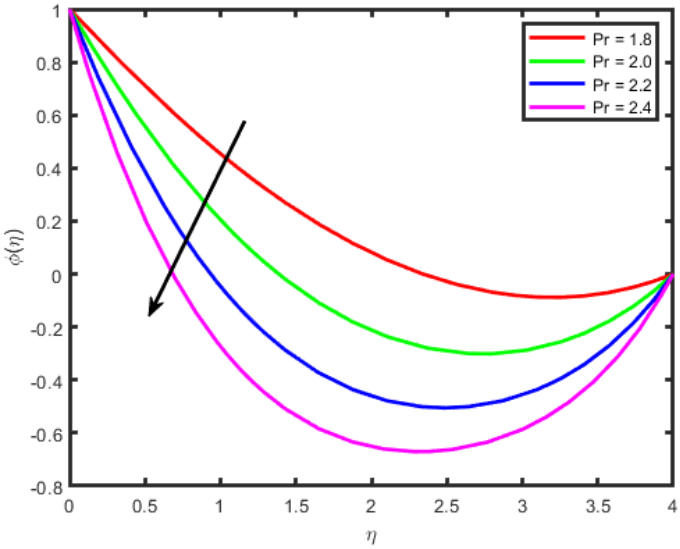

Fig. 13. Influence of Pr on ϕ(η)

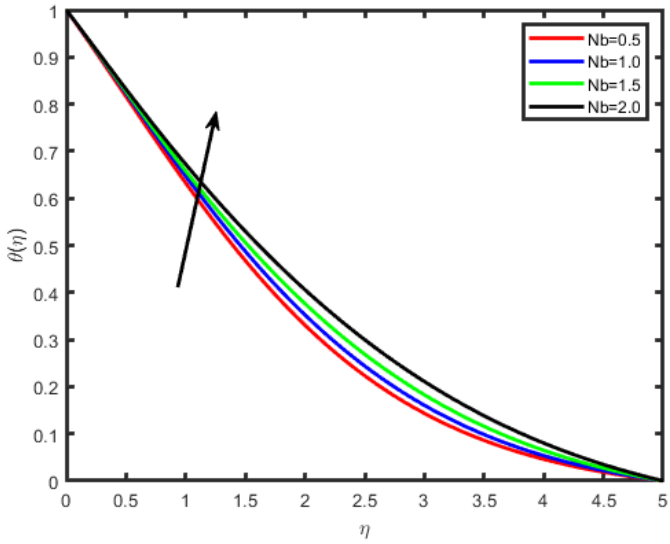

Fig. 14. Influence of Nb on θ(η)

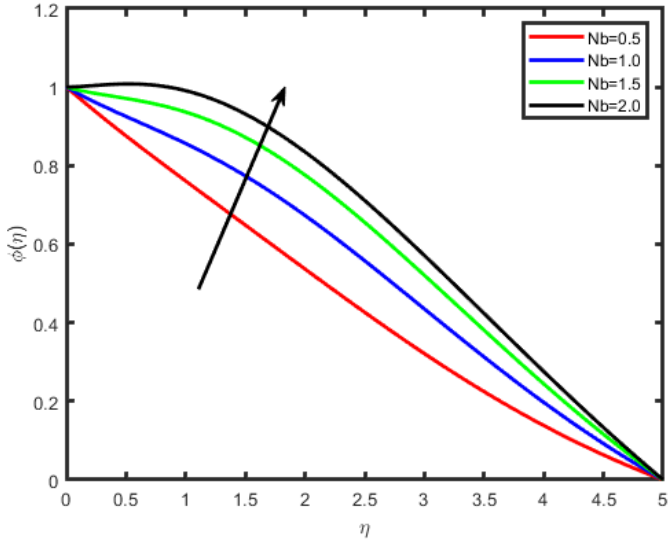

Fig. 15. Influence of Nb on ϕ(η)

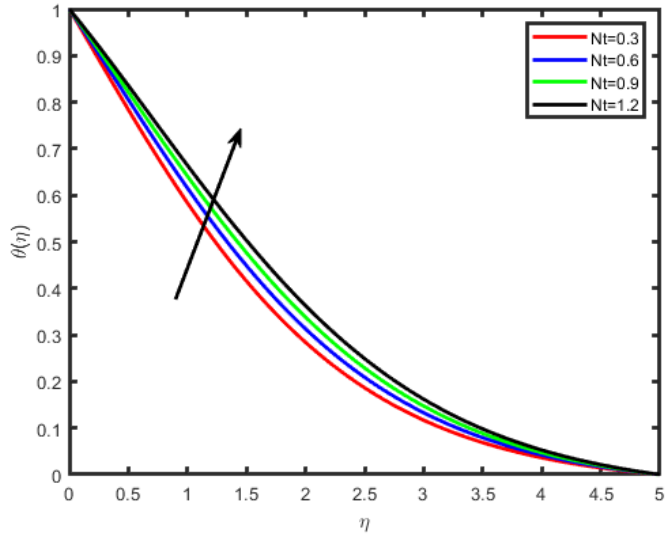

Fig. 16. Influence of Nt on θ(η)

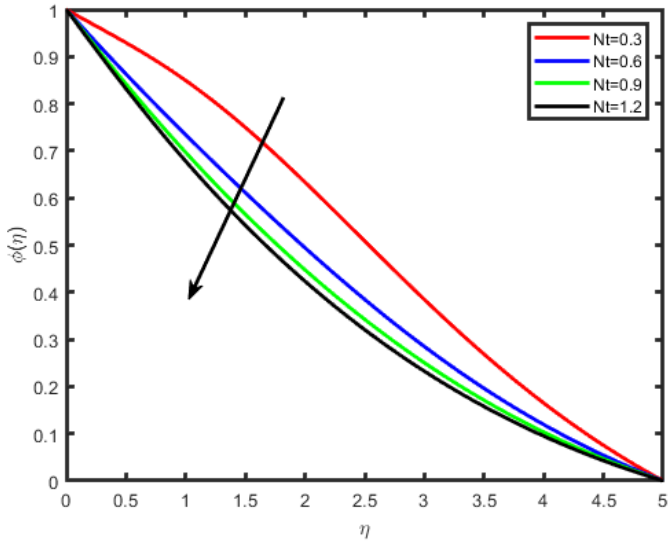

Fig. 17. Influence of Nt on ϕ(η)

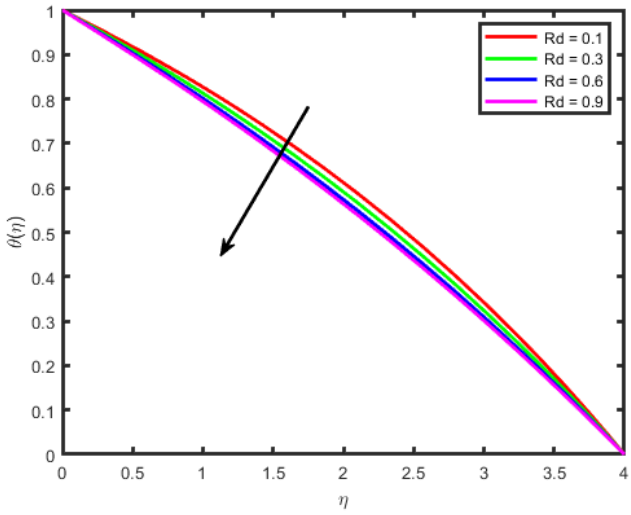

Fig. 18. Influence of Rd on θ(η)

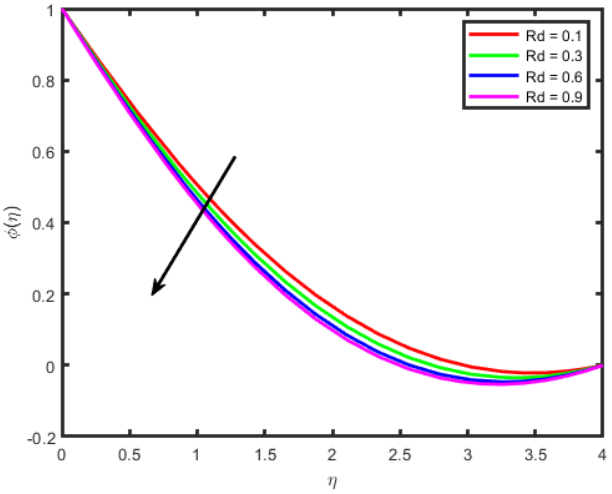

Fig. 19. Influence of Rd on ϕ(η)

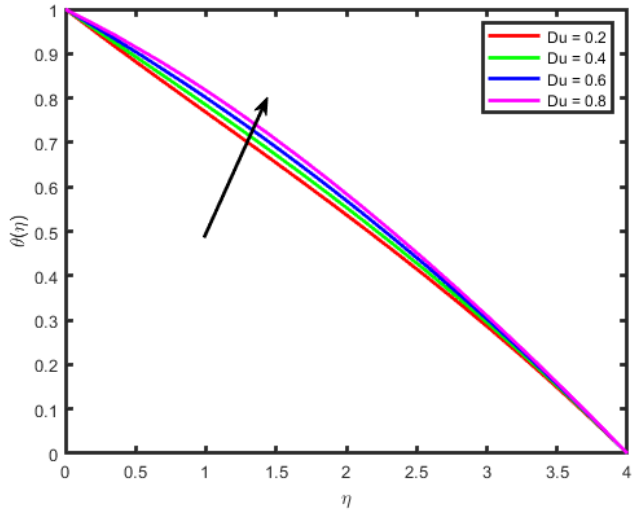

Fig. 20. Influence of Du on θ(η)

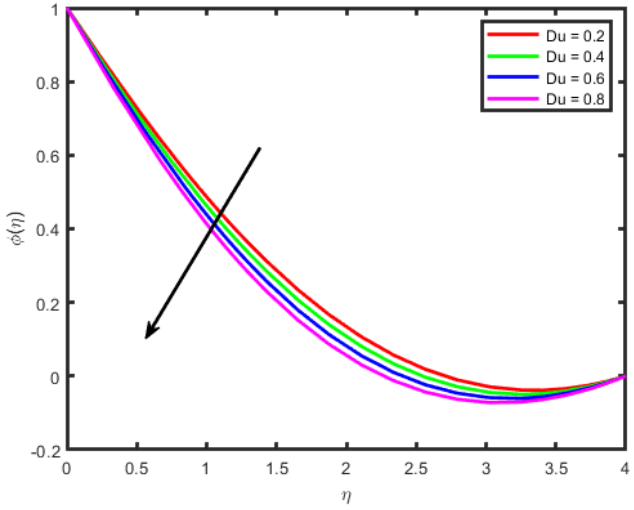

Fig. 21. Influence of Du on ϕ(η)

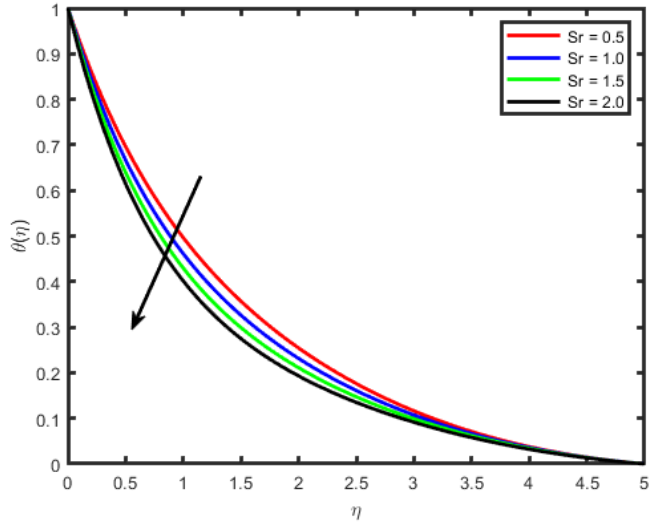

Fig. 22. Effect of Sr on θ(n)

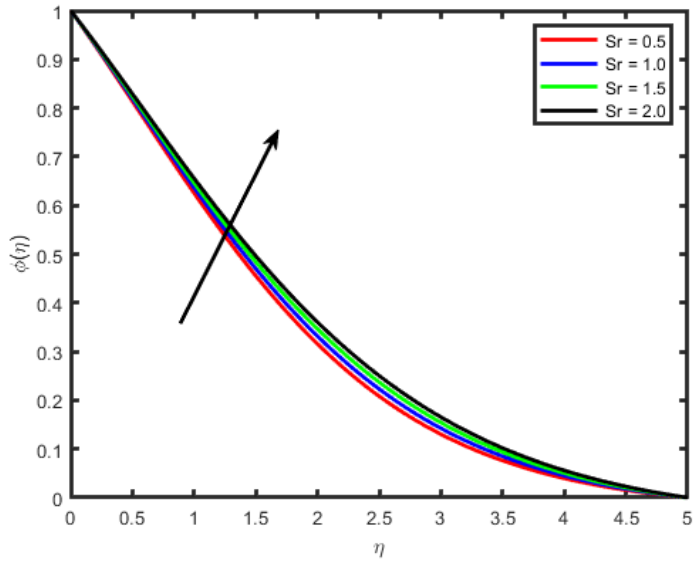

Fig. 23. Effect of Sr on ϕ(n)

Table 1 shows the Comparison of the presently computed values of wall temperature gradient $-\theta^{l}(0)$ with those of Bilal *et al.,* [11]. The Numerical results of the local Nusselt and Sherwood numbers for various values of different parameters are tabulated in Table 2. From Table 2, it is observed that the rate of heat flux decreases for the increasing values of Deborah number Λ and magnetic parameter M. It happens due to the fact that an increase in the magnetic parameter will enhance the Lorentz force which slows down the motion of the fluid and resultantly the rate of heat flux is reduced. The same phenomenon is observed for the increasing value of Λ and M for the case of Sherwood number ϕl(0). An increment is observed in the rate of the heat flux for the thermal radiation parameter Rd, the temperature ratio parameter θ_w and the stretching ratio c. Similarly for temperature ratio parameter θw, thermal radiation parameter Rd and stretching ratio c, a decreasing trend is noticed for the mass transfer rate. The influence of the thermophoresis parameter Nt, Brownian motion parameter Nb, Prandtl number Pr, land the Lewis number Le on the rate of heat and mass transfer is also shown in Table 2. From the numerical values, it is noticeable that Nt, Nb and Le have a decreasing effect on Nusselt number while this increases for the increasing values of Prandtl number. On the other hand, Sherwood number decreases for the increasing thermophoresis parameter Nt, however the rate of mass transfer enhances for the increasing values of Nb, Pr and Le

Table 1
The comparison of the presently computed values of wall temperature gradient $-\theta^{l}(0)$ with those of Bilal *et al.,* [11]

Λ	c	Pr	Bilal *et al.,* [11]	Present study
1	0.5	2	1.01694	1.015478
0.5			2.296655	2.278547
1.0			2.243930	2.245785
1.5			2.19501	2.197521
	0.3		2.09403	2.047855
	0.6		2.31293	2.301247
	1.0		2.55918	2.564785
		4	1.60165	1601547
		7	2.24393	2.24578
		10	2.75508	2.721452

Table 2
The numerical results of the local Nusselt and Sherwood numbers for various values of different parameters

Λ	M	Rd	θ_w	Sr	Nt	Nb	Pr	Du	Le	Nu_z	Sh_z
1.0	2.0	1.0	1.5	0.5	1.2	0.8	0.2	0.5	1.0	1.578521	0.7542141
0.2										1.495214	0.714245
0.4										1.401547	0.648752
0.6										1.364587	0.614578
	0.5									1.245775	0.612478
	1.0									1.002544	0.607247
	1.5									0.895475	0.601247
		0.1								0.787852	0.354785
		0.3								0.894578	0.547851
		0.6								0.942147	0.754782
			1.2							0.898542	0.354785
			1.4							0.987524	0.547852
			1.6							1.125878	0.745214
				0.5						1.078541	0.654785
				1.0						1.987852	0.697852
					0.5					1.345785	0.987852
					1.0					1.297854	0.854578
						0.3				1.457851	0.785452
							0.6			1.120124	0.987852
								0.2		0.785452	0.457852
								0.4		0.794521	0.403214
									1.0	1.245785	0.647851
									1.2	1.124785	0.874512

5. Concluding Remarks

This study investigated the influence of Diffusion thermo and thermal diffusion effects of non-linear thermal radiation of electrically conducting upper convected Maxwell fluid over a bi-directional stretching surface. Non-linear differential equations are solved numerically by shooting method with fourth order Runge-Kutta integration technique. The main features of the study are as follows:

i. UCM fluids have lower boundary layer thickness as compared to Newtonian fluid.
ii. Nusselt and Sherwood number both are gradually increased when temperature ratio is enhanced.
iii. Nanoparticle concentration decreases for Nb and increases for Nt.
iv. Flow velocity decreases for increasing value of thermal radiation parameter, the reversal behavior has observed in the case of diffusion thermo specification.
v. An increase in thermal boundary layer thickness is observed in temperature and concentration profiles.

References

[1] Bird, Robert Byron, Robert Calvin Armstrong, and Ole Hassager. "Dynamics of polymeric liquids. Vol. 1: Fluid mechanics." (1987).
[2] Fosdick, R. L., and K. R. Rajagopal. "Anomalous features in the model of “second order fluids”." *Archive for Rational Mechanics and Analysis* 70 (1979): 145-152. https://doi.org/10.1007/BF00250351
[3] Hayat, T., Z. Abbas, and M. Sajid. "Series solution for the upper-convected Maxwell fluid over a porous stretching plate." *Physics Letters A* 358, no. 5-6 (2006): 396-403. https://doi.org/10.1016/j.physleta.2006.04.117

[4] Sadeghy, Kayvan, Amir-Hosain Najafi, and Meghdad Saffaripour. "Sakiadis flow of an upper-convected Maxwell fluid." *International Journal of Non-Linear Mechanics* 40, no. 9 (2005): 1220-1228. https://doi.org/10.1016/j.ijnonlinmec.2005.05.006

[5] Rajagopal, Kumbakonam R., A. S. Gupta, and Alan S. Wineman. "On a boundary layer theory for non-Newtonian fluids." *International Journal of Engineering Science* 18, no. 6 (1980): 875-883. https://doi.org/10.1016/0020-7225(80)90035-X

[6] Mohamadali, Meysam, and Nariman Ashrafi. "Similarity solution for high Weissenberg number flow of upper-convected maxwell fluid on a linearly stretching sheet." *Journal of Engineering* 2016 (2016). https://doi.org/10.1155/2016/9718786

[7] Mushtaq, A., S. Abbasbandy, M. Mustafa, T. Hayat, and A. Alsaedi. "Numerical solution for Sakiadis flow of upper-convected Maxwell fluid using Cattaneo-Christov heat flux model." *AIP Advances* 6, no. 1 (2016). https://doi.org/10.1063/1.4940133

[8] Omowaye, Adeola John, and Isaac Lare Animasaun. "Upper-convected maxwell fluid flow with variable thermo-physical properties over a melting surface situated in hot environment subject to thermal stratification." *Journal of applied fluid mechanics* 9, no. 4 (2016): 1777-1790. https://doi.org/10.18869/acadpub.jafm.68.235.24939

[9] Krupalakshmi, Koneri L., Bijjanal J. Gireesha, Basavarajappa Mahanthesh, and Rama Subba Reddy Gorla. "Influence of nonlinear thermal radiation and Magnetic field on upper-convected Maxwell fluid flow due to a convectively heated stretching sheet in the presence of dust particles." *Communications in Numerical Analysis* 1 (2016): 57-73. https://doi.org/10.5899/2016/cna-00254

[10] I. Waini, N. A. Zainal, and N. S. Khashi'ie, "Aligned magnetic field effects on flow and heat transfer of the upper-convected Maxwell fluid over a stretching/shrinking sheet," MATEC Web Conferences, vol. 97, p. 01078, 2017. https://doi.org/10.1051/matecconf/20179701078

[11] Bilal, M., M. Sagheer, and S. Hussain. "On MHD 3D upper convected Maxwell fluid flow with thermophoretic effect using nonlinear radiative heat flux." *Canadian Journal of Physics* 96, no. 1 (2018): 1-10. https://doi.org/10.1139/cjp-2017-0250

[12] Raghunath, Kodi, Ravuri Mohana Ramana, Charankumar Ganteda, Prem Kumar Chaurasiya, Damodar Tiwari, Rajan Kumar, Dharam Buddhi, and Kuldeep Kumar Saxena. "Processing to pass unsteady MHD flow of a second-grade fluid through a porous medium in the presence of radiation absorption exhibits Diffusion thermo, hall and ion slip effects." *Advances in Materials and Processing Technologies* (2023): 1-18. https://doi.org/10.1080/2374068X.2023.2191450

[13] Kodi, Raghunath, Charankumar Ganteda, Abhishek Dasore, M. Logesh Kumar, G. Laxmaiah, Mohd Abul Hasan, Saiful Islam, and Abdul Razak. "Influence of MHD mixed convection flow for maxwell nanofluid through a vertical cone with porous material in the existence of variable heat conductivity and diffusion." *Case Studies in Thermal Engineering* 44 (2023): 102875. https://doi.org/10.1016/j.csite.2023.102875

[14] Raghunath, Kodi, Mopuri Obulesu, and Konduru Venkateswara Raju. "Radiation absorption on MHD free conduction flow through porous medium over an unbounded vertical plate with heat source." *International Journal of Ambient Energy* (2023): 1-9. https://doi.org/10.1080/01430750.2023.2181869

[15] Li, Shuguang, Kodi Raghunath, Ayman Alfaleh, Farhan Ali, A. Zaib, M. Ijaz Khan, Sayed M. ElDin, and V. Puneeth. "Effects of activation energy and chemical reaction on unsteady MHD dissipative Darcy–Forchheimer squeezed flow of Casson fluid over horizontal channel." *Scientific Reports* 13, no. 1 (2023): 2666.. https://doi.org/10.1038/s41598-023-29702-w

[16] Suresh Kumar, Y., Shaik Hussain, K. Raghunath, Farhan Ali, Kamel Guedri, Sayed M. Eldin, and M. Ijaz Khan. "Numerical analysis of magnetohydrodynamics Casson nanofluid flow with activation energy, Hall current and thermal radiation." *Scientific Reports* 13, no. 1 (2023): 4021. https://doi.org/10.1038/s41598-023-28379-5

[17] Ganjikunta, Aruna, Hari Babu Kommaddi, Venkateswarlu Bhajanthri, and Raghunath Kodi. "An unsteady MHD flow of a second-grade fluid passing through a porous medium in the presence of radiation absorption exhibits Hall and ion slip effects." *Heat Transfer* 52, no. 1 (2023): 780-806. https://doi.org/10.1002/htj.22716

[18] Pantokratoras, Asterios, and Tiegang Fang. "Sakiadis flow with nonlinear Rosseland thermal radiation." *Physica Scripta* 87, no. 1 (2012): 015703. https://doi.org/10.1088/0031-8949/87/01/015703

[19] Kodi, Raghunath, Mohana Ramana Ravuri, V. Veeranna, M. Ijaz Khan, Sherzod Abdullaev, and Nissren Tamam. "Hall current and thermal radiation effects of 3D rotating hybrid nanofluid reactive flow via stretched plate with internal heat absorption." *Results in Physics* 53 (2023): 106915. https://doi.org/10.1016/j.rinp.2023.106915

[20] Kodi, Raghunath, Ramachandra Reddy Vaddemani, M. Ijaz Khan, Sherzod Shukhratovich Abdullaev, Attia Boudjemline, Mohamed Boujelbene, and Yassine Bouazzi. "Unsteady magneto-hydro-dynamics flow of Jeffrey fluid through porous media with thermal radiation, Hall current and Soret effects." *Journal of Magnetism and Magnetic Materials* 582 (2023): 171033. https://doi.org/10.1016/j.jmmm.2023.171033

[21] Raghunath, Kodi. "Study of Heat and Mass Transfer of an Unsteady Magnetohydrodynamic (MHD) Nanofluid Flow Past a Vertical Porous Plate in the Presence of Chemical Reaction, Radiation and Soret Effects." *Journal of Nanofluids* 12, no. 3 (2023): 767-776. https://doi.org/10.1166/jon.2023.1923

[22] Raghunath, K., R. Mohana Ramana, V. Ramachandra Reddy, and M. Obulesu. "Diffusion Thermo and Chemical Reaction Effects on Magnetohydrodynamic Jeffrey Nanofluid Over an Inclined Vertical Plate in the Presence of Radiation Absorption and Constant Heat Source." *Journal of Nanofluids* 12, no. 1 (2023): 147-156. https://doi.org/10.1166/jon.2023.1923

[23] Maatoug, Samah, K. Hari Babu, V. V. L. Deepthi, Kaouther Ghachem, Kodi Raghunath, Charankumar Ganteda, and Sami Ullah Khan. "Variable chemical species and thermo-diffusion Darcy–Forchheimer squeezed flow of Jeffrey nanofluid in horizontal channel with viscous dissipation effects." *Journal of the Indian Chemical Society* 100, no. 1 (2023): 100831. https://doi.org/10.1016/j.jics.2022.100831

[24] Bafakeeh, Omar T., Kodi Raghunath, Farhan Ali, Muhammad Khalid, El Sayed Mohamed Tag-ElDin, Mowffaq Oreijah, Kamel Guedri, Nidhal Ben Khedher, and Muhammad Ijaz Khan. "Hall current and Soret effects on unsteady MHD rotating flow of second-grade fluid through porous media under the influences of thermal radiation and chemical reactions." *Catalysts* 12, no. 10 (2022): 1233. https://doi.org/10.3390/catal12101233.

[25] Deepthi, V. V. L., Maha MA Lashin, N. Ravi Kumar, Kodi Raghunath, Farhan Ali, Mowffaq Oreijah, Kamel Guedri, El Sayed Mohamed Tag-ElDin, M. Ijaz Khan, and Ahmed M. Galal. "Recent development of heat and mass transport in the presence of Hall, ion slip and thermo diffusion in radiative second grade material: application of micromachines." *Micromachines* 13, no. 10 (2022): 1566. https://doi.org/10.3390/mi13101566.

[26] Ramzan, Muhammad, and Muhammad Bilal. "Time dependent MHD nano-second grade fluid flow induced by permeable vertical sheet with mixed convection and thermal radiation." *PloS one* 10, no. 5 (2015): e0124929. https://doi.org/10.1371/journal.pone.0124929

[27] Ibrahim, Wubshet. "Nonlinear radiative heat transfer in magnetohydrodynamic (MHD) stagnation point flow of nanofluid past a stretching sheet with convective boundary condition." *Propulsion and Power Research* 4, no. 4 (2015): 230-239. https://doi.org/10.1016/j.jppr.2015.07.007